



Environmental
Science
Nano

Optimizing the synergistic effect of CuWO₄/CuS hybrid composites for photocatalytic inactivation of pathogenic bacteria

Journal:	<i>Environmental Science: Nano</i>
Manuscript ID	EN-ART-04-2022-000361.R2
Article Type:	Paper

SCHOLARONE™
Manuscripts

Environmental Significance

Microbial contamination poses a serious risk in water resources worldwide. Despite considerable progress on the development of hybrid photocatalytic semiconductors for wastewater treatment and disinfection applications, very little is currently known about how to optimize the synergistic effect between two different semiconductor photocatalysts. In this study, for the first time, the broth microdilution checkerboard assay was adapted to systematically evaluate the antibacterial efficacy of nanopowders of CuWO_4 and CuS individually in comparison with hybrid composites prepared by mixing CuWO_4 and CuS with varying weight ratios. This method provided a way to find the best and most effective combination of antimicrobial photocatalysts. These findings have significant implications for controlled coupling of two or more semiconductors with suitable bandgaps to develop new and effective antimicrobial materials for water disinfection.

ARTICLE

Optimizing the synergistic effect of CuWO₄/CuS hybrid composites for photocatalytic inactivation of pathogenic bacteria

Received 00th January 20xx,
Accepted 00th January 20xx

Xiuli Dong,^{†¶a} Rowan R. Katzbaer,^{‡b} Basant Chitara,^a Li Han,^c Liju Yang,^d Raymond E. Schaak,^{*b} and Fei Yan^{*a}

DOI: 10.1039/x0xx00000x

Herein, we report an effective strategy to maximize the antimicrobial activity of CuWO₄/CuS hybrid composites, prepared by simply mixing CuWO₄ and CuS nanopowders with varying weight ratios in phosphate buffered saline solution by ultrasound. The tested bacteria included gram negative (G⁻) pathogenic bacteria *Salmonella typhi*, gram positive (G⁺) pathogenic bacteria *Staphylococcus aureus*, and G⁺ bacteria *Bacillus subtilis*. The as-prepared composites exhibited much enhanced antibacterial efficiency compared with individual CuWO₄ and CuS nanopowders under white light irradiation. The checkerboard array analysis revealed that the combination of 8 µg/mL CuWO₄ and 2 µg/mL CuS was most efficient and generated the optimal synergistic effect, showing a complete killing effect on all the tested bacteria from 3 strains with ~ 5.8 log cell reduction. The significantly enhanced catalytic efficiency can be ascribed to the formation of a type-II heterojunction between CuWO₄ and CuS, which can effectively improve the charge separation efficiency and increase the light absorption. Moreover, the hybrid composites prepared by ultrasound-assisted physical mixing can effectively increase interface area, which greatly facilitates the charge mobility and transfer in the interfaces between CuWO₄ and CuS. This study offers new insights into the integration of different semiconductors to optimize their synergistic effect on antimicrobial activities for water disinfection.

1. Introduction

Pathogens are the leading cause of many infectious diseases and developing antibacterial materials is a priority for global health. There are an estimated 31 major pathogens acquired in the United States each year, causing 9.4 million episodes of foodborne illness, about 55,000 hospitalizations, and over 1000 deaths.¹ In these outbreaks, *Staphylococcus aureus* (*S. aureus*) caused 3% of foodborne illnesses, and *Salmonella spp.* caused 28% of deaths.^{1, 2} The treatment of bacterial infections can be difficult when an antibiotic resistant function was developed in these bacteria. It has been reported that mutant antibiotic resistant strains such as Methicillin Resistant *S. aureus* (MRSA) have been transmitted rapidly through hospital facilities and personal care products, leading to an uncontrollable problem.³ Moreover, some environmental pathogens, such as *Bacillus anthracis* (*B. anthracis*), have been used as biological weapons by terrorists. *B. anthracis*, the etiologic agent of anthrax, is a

Gram positive spore-forming bacterium.⁴ *B. anthracis* spores could enter the human or animal's body through skin lesion, lungs, or gastrointestinal route and cause severe illness.⁴

Many traditional antimicrobial reagents have been used to inactivate pathogenic bacteria. However, these chemicals are often toxic, creating potentially major issues in environmental and ecological systems and raising public health concerns.⁵ As one of the new promising antimicrobial strategies, photocatalysis has emerged as an effective green solution for disinfection applications. The antimicrobial effect of photocatalysts was first found in titanium dioxide (TiO₂) by Mastunaga et al. in 1985.⁸ Unfortunately, TiO₂ only absorbs the UV light which accounts for a small fraction (~ 4%) of the entire solar spectrum.⁹ Some photocatalysts, such as graphitic carbon nitride (g-C₃N₄)⁶ and hybrid graphene oxide-silver nanoparticle composites,⁷ have been reported to be able to inactivate antibiotic-resistant bacteria under visible light irradiation.⁶ Thus, it is of great interest to develop photocatalysts that can yield high reactivity under visible light so that a great portion (~ 45%) of the solar spectrum is utilized in photocatalytic destruction of bacteria.⁹

Copper tungstate (CuWO₄) is an efficient visible light responsive photocatalyst with unique properties, including eco-friendliness, low cost, optimum band edge potentials, as well as remarkable stability under oxidative and acidic conditions.¹⁰ Benko et al.¹¹ first reported the photoelectrochemical properties of CuWO₄ in 1982. Since then, many efforts have been made to improve its photocatalytic and photoelectrochemical performance. One such strategy to

^a Department of Chemistry and Biochemistry, North Carolina Central University, Durham, NC 27707, USA. Email: fyan@nccu.edu; xdong@campbell.edu; res20@psu.edu

^b Department of Chemistry, The Pennsylvania State University, University Park, PA 16802, USA.

^c RTI International, Research Triangle Park, NC 27709, USA

^d Department of Pharmaceutical Sciences, North Carolina Central University, Durham, NC 27707, USA.

[†] Electronic Supplementary Information (ESI) available: See

DOI: 10.1039/x0xx00000x

[‡] Equal contribution.

[¶] Current address: School of Osteopathic Medicine, Campbell University, Lillington, NC 27506.

improve the photocatalytic performance of CuWO_4 is to create a composite material with a photocathode, as CuWO_4 has the appropriate conduction band energy to act as a photoanode for the oxygen evolution half-reaction of water.^{12,13} Its conduction band edge potential is more positive than that of CuO .¹⁴

Several studies have reported that CuWO_4 shows antimicrobial effects. For instance, it was reported that CuWO_4 demonstrated strong antimicrobial activity against *Candida albicans* and *S. aureus* by the disk diffusion assay.¹⁵ Gupta et al.¹⁶ synthesized the Z-scheme composite $\text{g-C}_3\text{N}_4/\text{CuWO}_4$, which showed the photocatalytic degradation of *S. aureus* and *E. coli* bacteria with 0.9 and 1.15 log reduction, respectively. Vignesh et al.¹⁷ synthesized CdS and CuWO_4 modified TiO_2 nanoparticles, displaying a strong inactivation effect on *P. aeruginosa*.

Copper sulphide (CuS) is another visible-light-driven photocatalyst. Nonporous CuS exhibits excellent photocatalytic activity on the degradation of methylene blue (MB), methyl orange (MO), and rhodamine B (RhB).¹⁸ CuS also shows excellent antimicrobial activity against bacteria such as *S. aureus* and *E. coli*.¹⁹ Antimicrobial effects were also observed for CuS nanocrystals modified with different moieties, including Au ,²⁰ lysozyme,²¹ L-alanine and L-aspartic acid,²² etc. It was reported that Au@CuS core-shell nanoparticles were highly effective to inhibit the growth of *B. anthracis* vegetative cells.²⁰

To enhance the performance of photocatalysts, the most common strategy is to form the heterojunction structure with other semiconductors. The generation of new heterojunctions by semiconductors with different bandgap energy and band edge potentials is beneficial for the separation and stabilization of photogenerated electrons and holes, can adjust the absorption range of light to lower energy, and facilitate the photocatalysis process.²³⁻²⁶ However, it is a significant challenge to optimize the composition of these semiconductors to achieve maximum efficiency. In the area of medical science, a broth microdilution checkerboard method has been used to evaluate the antimicrobial synergistic effect of the combination of two drugs *in vitro*.²⁷ In the checkerboard assay, two antimicrobial drugs are tested in 2-fold serial dilutions with all possible combinations in 96-well plates. The results can be used to determine the interaction of the two drugs and provide the optimal combinations. It might be feasible to use this method with some modifications to optimize the antimicrobial synergistic effect of a hybrid composite that consists of two different semiconductor photocatalysts with varying weight ratios.

In this work, CuWO_4 was synthesized via a solid-state reaction. The antimicrobial activity of hybrid composites, which were prepared by mixing CuWO_4 and CuS with varying weight ratios in PBS buffer solution by ultrasound, was examined under the irradiation of a white light (60 W). The tested bacteria included gram negative (G^-) bacteria *Salmonella typhi* (*S. typhi*), gram positive (G^+) bacteria *S. aureus*, and G^+ bacteria *Bacillus subtilis* (*B. subtilis*) which were used as a surrogate of pathogenic *B. anthracis*. To the best of our knowledge, there is only one other report on the fabrication of CuWO_4/CuS hybrid composites by physical mixing, used for photodegradation of RhB.²⁸ It is anticipated that the as-prepared composite will be able to

broaden the light response range, prolong the life of photogenerated electrons and holes, and enhance photocatalytic activity of CuWO_4 . This approach is poised to find optimal semiconductor combinations for pathogen disinfection. This is the first instance that the modified broth microdilution checkerboard assay was used to optimize the synergistic effect of two different semiconductors for antimicrobial activity.

2. Materials and methods

2.1 Chemicals

CuS (99.8% purity) and WO_3 (99.8% purity) were purchased from Alfa Aesar. CuO (>99% purity) and isopropanol were purchased from Sigma Aldrich (St. Louis, MO). *S. typhi*, *S. aureus*, and *B. subtilis* were purchased from the American Type Culture Collection (ATCC; Manassas, VA).

2.2 Synthesis of CuWO_4

The bulk CuWO_4 powder was synthesized from stoichiometric amounts of CuO and WO_3 . The powders were ground together, placed in an alumina crucible, and fired in air at 800 °C for 24 hours.

2.3 Characterization

2.3.1 Powder X-ray diffraction

The powder X-ray diffraction (PXRD) scans were performed on a Malvern Panalytical XPert Pro MPD instrument with a copper source, using line focus and reflection mode. Simulated patterns were calculated from data retrieved from Springer Materials.

2.3.2 Scanning electron microscopy/energy-dispersive X-ray spectroscopy

CuWO_4 and CuS powders were suspended in water by probe sonication (Qsonic, XL-2000 series, output wattage at 6) for 10 minutes. The prepared suspensions were dropcast onto SEM silicon wafer and allowed to dry for imaging. Scanning electron microscopy (SEM) images were collected with an FEI Quanta 200 Environmental scanning electron microscope. Energy-dispersive X-ray spectroscopy (EDS) data of the sample were collected at 20 kV on a ESEM Q250 with a tungsten source equipped with a S10 EDS Bruker AXS detector. Secondary electrons were used to map elemental composition in low vacuum mode. Oxford Instruments AZtec software was used to assign peaks in the EDS spectra. EDS quantification was also performed using the AZtec software package; atomic percentages were determined through peak integration.

2.3.3 UV-Vis spectroscopy

A Perkin Elmer Lambda 950 UV-Vis-NIR spectrometer was used to measure diffuse reflectance spectra using a 150 mm integrating sphere, in diffuse reflection mode. Spectra were collected from 250-2500 nm, with 2 nm steps. The reference spectrum for total

reflectance was measured against a Spectralon disc standard. Samples were suspended in ethanol and drop cast on quartz glass slides (Electron Microscopy Sciences). The slides were dried with nitrogen before measurement. Plots of the Kubelka-Munk function, raised to the power two, vs. energy in eV were constructed. Bandgaps were calculated by fitting the linear region in the onset of absorption and extrapolating to the x-intercept.

2.3.4 Surface area measurements

The Brunauer–Emmett–Teller (BET) surface area was measured by the nitrogen adsorption isotherms measurements (Micromeritics ASAP 2020). The samples were degassed for two hours at 90 °C prior to measurement. A five-point nitrogen adsorption experiment was run and fit by a BET model to obtain the isotherms.

2.3.5 Photoluminescence spectroscopy

The photoluminescence (PL) measurements were performed using a Raman spectrometer (Horiba LabRAM Evolution RAMAN microscope) with 532 nm laser excitation.

2.4 Antimicrobial assays

2.4.1 Bacteria preparation

Three bacterium strains were used in this study, including *S. typhi*, *S. aureus*, and *B. subtilis*. Fresh grown bacterial cells were used for each treatment of photocatalysts. For the preparation of bacterial cells, single colonies were inoculated in tryptic soy broth (TSB) and grew at 37°C on a shaker for 12 h. The cells were collected in the mid-log phase of the culture with the value of optical density (OD) ~ 0.6 at the wavelength of 595 nm. TSB medium was then removed and the cells were washed twice with phosphate-buffered saline (PBS) by centrifugation (8,000 rpm, 5 min). The cells were re-suspended in PBS and diluted with PBS for later treatment. The cell concentration in each treatment was kept at ~ 5×10^5 colony-forming unit (cfu)/mL.

2.4.2 Antimicrobial test of CuWO₄ and CuS

The CuS and CuWO₄ suspensions were prepared in deionized (DI) H₂O and sonicated for 10 min before reaction preparations using an ultrasonic water bath (Branson Ultrasonics Corporation, Danbury, CT, USA). The bacteria treatments were performed in 96-well plates. The cells were treated with CuWO₄ and CuS alone or in combination with various concentrations in ½ PBS, which were prepared using 75 µL of cells in PBS and 75 µL of photocatalysts in DI-H₂O. The plates were placed on a shaker (Lab-Line Instruments, Inc., IL) at the setting of two and exposed to white light (60 W) at the distance of 5 cm for 1 h treatment at room temperature. For comparison, the dark treatment was also included at the same treatment condition as the light treatment, except that the plates were wrapped with aluminum foil to avoid light illumination. A series of 10-fold dilutions of CuS and CuWO₄ suspensions were performed immediately after the treatment with the bacterial cells with and without white light irradiation. No attempts were made to try to separate these particles from the cells. A 100 µL aliquot of each dilution was then used to spread on tryptic soy agar (TSA) plates. The viable cell numbers were

calculated based on the bacterial colony numbers after 18 h incubation at 37°C. Except for the duration of the light treatment, the whole procedure was carried out in the dark. The presence of highly diluted aqueous suspension of the CuS and CuWO₄ particles should have a negligible effect on the final bacterial CFU counts.

2.4.3 Checkerboard assay and fractional inhibitory concentration (FIC) index determination

To study whether there are synergistic antimicrobial interactions between CuWO₄ and CuS and to find the most effective CuWO₄/CuS combination, a checkerboard method was used, similar to the traditional broth microdilution checkerboard method with some modifications.²⁴ The experiment was performed in 96-well plates. Aliquots of 50 µL *S. typhi* cells in PBS were added into all the wells. CuWO₄ and CuS suspensions with two-fold serial dilutions were prepared in DI-H₂O separately, and then were added into the wells at a volume of 25 µL to achieve two-fold serial dilutions with desired concentrations along the abscissa and ordinate of the plate, respectively, with a final reaction volume of 100 µL in each well. The resulting checkerboard contained all the possible combinations of the prepared CuWO₄ and CuS suspensions, plus CuWO₄ and CuS alone. The plates were placed on the shaker and exposed to light for 1 h at room temperature. TSB at a volume of 100 µL was then added into each well. OD595 values were measured as growth time 0 using SpectraMas M5 multidetection reader (Molecular Devices LLC, Sunnyvale, CA, USA) and the plates with the same reactions but without bacterial cells were used as blanks. The plates were incubated at 37 °C in the dark for 18 h, the reactions were homogenized by pipetting up and down for at least 10 times, and OD595 values were tested at a growth time of 18 h. The increase in OD595 values after growths indicated bacterial growth.

The minimal inhibitory concentration (MIC) of each semiconductor was defined as the lowest concentration that completely inhibited the bacterial growth. The FIC index (Σ FIC) was calculated by the use of following equation:

$$\Sigma \text{FIC} = A/\text{MIC}_A + B/\text{MIC}_B = \text{FIC}_A + \text{FIC}_B \quad (1)$$

where A and B are the MIC of each hybrid composite (in a single well), and MIC_A and MIC_B are the MIC of individual semiconductor nanocrystal.²⁹

The interaction between the two combined reagents was determined by the Σ FIC values as follows: Σ FIC ≤ 0.5 indicates synergy, 0.5 < Σ FIC ≤ 0.75 indicates partial synergy, 0.75 < Σ FIC ≤ 1 indicates additive, 1.0 < Σ FIC < 4.0 indicates indifference, and Σ FIC ≥ 4.0 indicates antagonism.^{5, 30-32}

2.4.4 Isobologram analysis

To graphically visualize the interactions of CuWO₄ and CuS on *S. typhi* bacteria, an isobologram was plotted based on the results of checkerboard assays. In the isobologram, the concentrations of CuS and CuWO₄ from the growth-no growth interface were plotted on the x- and y-axis, respectively, and then the MIC of each nanocrystal alone was plotted and joined by a line on the graph. It was considered as additive interactions if the combination line fell along the line connecting the two MIC

values, as synergistic interactions if the combination line fell below, and as antagonistic interactions if the combination line was concave-up.^{33,34}

2.4.5 Antimicrobial test of CuWO₄/CuS hybrid composites

Hybrid composites of CuWO₄/CuS with different weight ratios were used to treat three bacterial strains, including *S. typhi*, *S. aureus*, and *B. subtilis*. The concentrations of CuWO₄ and CuS were determined according to the checkerboard results on *S. typhi* and the most effective combination was used together with other combinations for 1 h light treatment. In this way, the most effective combination can be confirmed and optimized. After the treatment, viable cell numbers were tested on TSA plates using the plating methods.

3. Results and discussion

3.1 Characterization of CuWO₄ and CuS

3.1.1 Powder XRD analysis

PXRD patterns of as-prepared CuWO₄ and as-purchased CuS are shown in Fig. 1. The diffraction peaks observed in both samples are identical to simulated patterns for the triclinic phase of CuWO₄³⁵ and hexagonal covellite CuS.³⁶ All peaks matched the reference pattern, and no impurity phases could be observed.

3.1.2 UV-Vis diffusive reflectance spectroscopy

The light absorption properties of CuWO₄ and CuS were examined using ultraviolet-visible diffuse reflectance spectroscopy. Fig. 2 illustrates the UV-Vis diffuse reflectance spectra of CuWO₄ and CuS. The optical bandgaps of these two materials were calculated using plots of the Kubelka-Munk function³⁵⁻³⁷ vs. energy in eV. These materials possess a direct band gap and so the function is raised to the power of two. Bandgaps were calculated by fitting the linear region in the onset of absorption and extrapolating to the x-intercept. The calculated band gap values were determined to be 2.4 and 1.8 eV for CuWO₄ and CuS, respectively. These values match well with those previously reported in literature.³⁸ This indicated that both materials are photosensitive to visible light.

3.1.3 Scanning Electron Microscopy/Energy-Dispersive X-ray Spectroscopy

The morphologies of these two materials were observed by SEM. SEM images (Fig. 3) reveal that CuWO₄ and CuS are polycrystalline with various shapes and that a majority of the crystallites have dimensions ranging from 10 nm to 300 nm. Elemental analysis was performed by energy-dispersive X-ray spectroscopy (EDS) and the spectra for CuWO₄ and CuS are shown in Fig. 3b and Fig. 3d, respectively. The EDS spectra confirm the presence of copper (Cu), tungsten (W), and oxygen (O) in CuWO₄, and the presence of Cu and sulphur (S) in CuS. All samples did exhibit a background oxygen and carbon (C) signal from the carbon tape substrate. Subtracting the roughly 10 atomic percent of oxygen signal from the carbon tape, it is

found that the Cu:W:O ratio of CuWO₄ corresponds to the expected 1:1:4 ratio. Similarly, CuS exhibits a Cu:S ratio of 1:1.

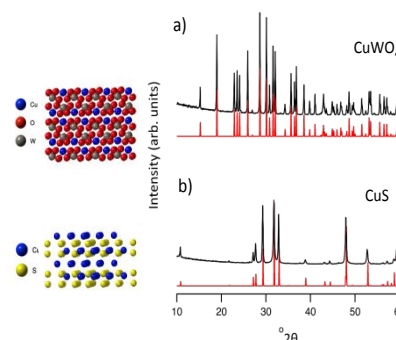


Fig. 1 XRD patterns of a) CuWO₄, and b) CuS

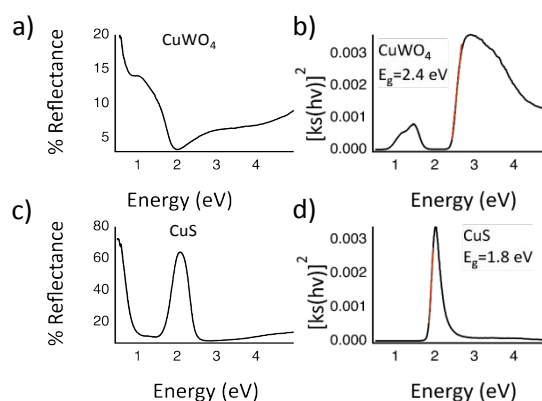


Fig. 2. UV-Vis diffuse reflectance spectra for a) CuWO₄ and c) CuS, and corresponding direct bandgap calculation: b) CuWO₄ and d) CuS utilizing the Kbelka-Munk function.

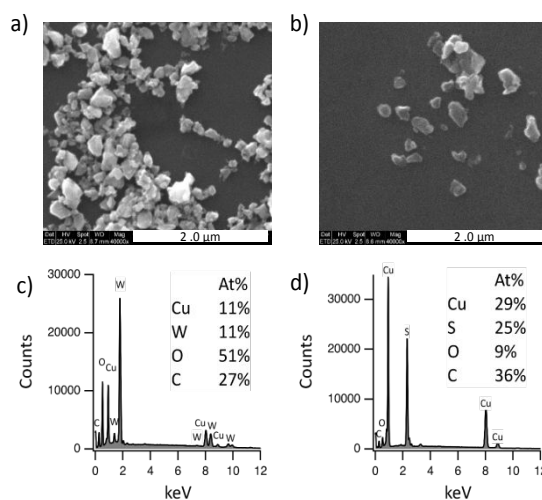


Fig. 3 SEM images of a) CuWO₄ and b) CuS, and their corresponding EDS spectra. Scale bar: 2.0 μm.

3.2 Antimicrobial assays of pure CuWO₄ and CuS

3.2.1 Antimicrobial effects of CuWO₄ and CuS

Fig. 4a shows the antimicrobial effects of CuWO₄ on *S. typhi* cells after treatment with 8, 16, 32, and 64 µg/mL CuWO₄ for 1 h under visible light illumination or in the dark. With light illumination, CuWO₄ showed concentration-dependent antimicrobial effects. When the CuWO₄ concentration was 8 µg/mL, a 0.5 log reduction in bacteria population. When the CuWO₄ concentration was increased to 64 µg/mL, there was complete inactivation of the bacteria, with no viable cells detected, a 5.58 log reduction. In contrast, CuWO₄ did not show obvious antimicrobial effect in the dark, even at the concentration of 64 µg/mL, which confirms that this is a photocatalytic process. This observation was consistent with previous studies, which reported the antimicrobial effects of CuWO₄ on bacteria and fungi (*Candida albicans* and *Aspergillus niger*) by disc diffusion methods.¹⁵ As for the antibacterial effect comparison of this study with what was reported by others, there were no prior publications that provided the concentration range of CuWO₄ with antimicrobial effects.

The antimicrobial activity of CuWO₄ depends on several factors, including its degree of agglomeration, molecular weight, nutrient composition, host, natural nutrient constituency, solvent, target microorganism, and physicochemical properties, and is inversely affected by pH.^{15,39} Besides the limited application study of CuWO₄ on antimicrobial effects, CuWO₄ has been utilized to photodegrade hazardous organic and inorganic pollutants, demonstrating excellent activity towards the degradation of ciprofloxacin,⁴⁰ MO,⁴¹ MB,⁴² tetracycline antibiotic,⁴³ terephthalic acid,⁴⁴ among other pollutants. Other applications of CuWO₄ included photocatalytic water reduction for H₂ generation and photoelectrochemical water splitting.¹⁰

Fig. 4b shows the antimicrobial effects of individual CuS nanopowders on *S. typhi* cells. Similar to CuWO₄, the effects of CuS were light-activated and concentration-dependent. CuS showed

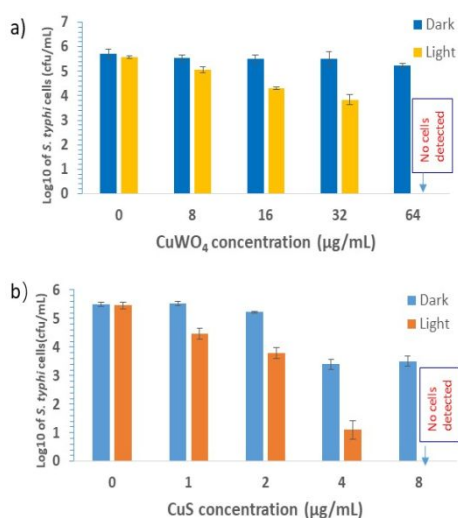


Fig. 4 Antimicrobial effects of CuWO₄ (a) and CuS (b) on *S. typhi* cells in the dark or under the light. Data is presented as mean values with ± SD error bars.

obvious antimicrobial effects even at the concentration of 1 µg/mL, displaying 1 log cell reduction after 1 h light treatment. Whereas, CuS at the concentration of 8 µg/mL completely killed bacteria with 5.5 log reduction. It is worth noting that CuS induces 1.5-2 log cell reduction at high concentrations such as 4 and 8 µg/mL even without light treatment. The antimicrobial effect of a photocatalyst under dark conditions is called dark toxicity or innate toxicity, which could be attributed to the presence of free metal ions released to the medium. Liang et al. found that a certain amount of Cu²⁺ could be released from CuS nanoparticles and Cu²⁺ could damage the structures of DNA, enzymes, and cell membranes, and affect biochemical properties, leading to bacterial death.¹⁹ Giachino and Waldron⁴⁵ reported that excess Cu²⁺ is extremely toxic and generated distinctive pleiotropic effects in the cells.²⁰ In our study, it is highly plausible that the Cu²⁺ release from CuS produced excess Cu²⁺ in the environment and caused bacteria death, displaying a cell concentration reduction after treatments in the dark.

Others also reported antimicrobial effects of CuS on bacteria. Liang et al.¹⁹ used CuS to treat *S. aureus* infected wounds on the back of rats and observed that CuS had antibacterial properties, and particularly, 500 µg/mL CuS had good antimicrobial effects without increasing side effects. The authors also indicated that CuS promoted wound healing through reepithelialization and collagen deposition.¹⁹ Malakodi and Rajeshkumar⁴⁶ synthesized CuS by using bacteria *Serratia nematodiphila* to reduce CuSO₄ into CuS and found that the MIC of CuS against *E. coli*, *S. aureus*, *K. pneumoniae*, and *P. vulgaris* was 30, 40, and 50 µg/mL, respectively. Huang et al.⁴⁶ utilized bovine serum albumin (BSA) as the template to synthesize CuS NPs and observed antimicrobial effects on *S. aureus* and *E. coli* cells after treated with 50 ppm BSA-CuS NPs under near infrared light.

The CuS used in this study was more effective than those used by others^{19, 42,47} possibly due to the difference in particle size, treatment condition, bacterium strain, etc. It has been demonstrated that CuS nanoparticles interact with the proteins and possible phospholipids associated with the proton pump of bacterial membranes, leading to a collapse of membrane proton gradient, a disruption of many cellular metabolisms, and cell deaths.^{48,49}

3.3 Interaction of CuWO₄ and CuS in combination

Combined treatment of two antimicrobial reagents is generally an effective strategy to inactivate bacteria and also fight resistance.⁵⁰ To find the most efficient CuWO₄/CuS combination and confirm the synergistic antimicrobial interactions between CuWO₄ and CuS, the checkerboard method was used to examine the inhibition of the growth of *S. typhi* cells treated with CuWO₄ and CuS separately and in combination. The most efficient combination in this study was considered as the one which could completely kill all the cells with the lowest concentration of CuWO₄ and CuS. Fig. 5 illustrates the setup of the checkerboard assay. The MICs of CuWO₄ and CuS were 64 and 8 µg/mL, respectively, showing consistency with the results tested by plating methods above. The FIC indexes were calculated (Table 1). The combination of 8

Table 1. Fractional inhibitory concentration (FIC) index and the interaction between CuWO₄ and CuS.

CuWO ₄ concentration(μg/mL)	CuS concentration(μg/mL)	ΣFIC	relation
64	0		MIC of CuWO ₄
32	0.25	0.53125	Partial synergy
8	2	0.375	Synergy
2	4	0.53125	Partial synergy
0	8		MIC of CuS

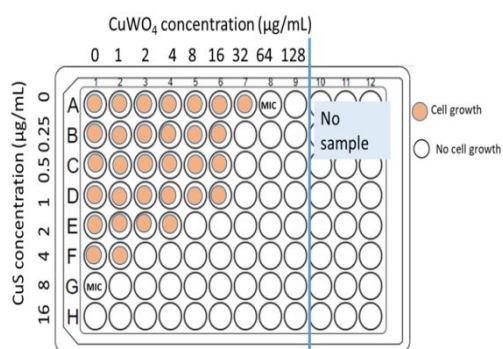
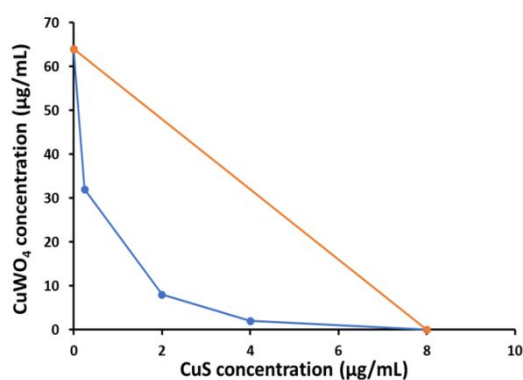
μg/mL CuWO₄ and 2 μg/mL CuS showed the ΣFIC value of 0.375, which was the lowest ΣFIC value among all the combinations, indicating this combination was the most efficient combination and the interaction between 8 μg/mL CuWO₄ and 2 μg/mL CuS was synergistic.

The other 2 combinations listed in the table were the combination of 32 μg/mL CuWO₄ with 0.25 μg/mL CuS, and the combination of 2 μg/mL CuWO₄ with 4 μg/mL CuS, showing partial synergistic interactions. A different result was observed on the synthesized CuWO₄/CuS heterojunction, which showed the best photocatalytic efficacy on the photodegradation of RhB at the ratio of 1:1.²⁸

The interaction between CuWO₄ and CuS in combination was further tested using isobologram. Isobolograms are an alternative method of interpretation of the interaction of two compounds on a defined microorganism and used when FIC gives borderline values.³³ Fig. 6 shows the line of MICs in CuWO₄/CuS combination fell below the line of MICs from CuWO₄ and CuS treatment alone, indicating the synergistic interaction between CuWO₄ and CuS. This observation proved the synergistic relation tested both by the plating method and by the checkerboard method.

Combination treatment of two antimicrobial reagents with synergistic interactions can reduce the frequency of drug resistance and minimize the dosage of toxic drugs, achieving more significant effects than monotherapy in biochemical activity.⁵¹ To achieve a maximal synergistic effect, the determinations of the reagent type, combination ratio, reaction

conditions, and screening methods are essential. The checkerboard method developed in this study was easy to handle and could provide sufficient data to find the most efficient combination and to optimize the ratios of two reagents. The major difference between the checkerboard assay in this study and the traditional broth microdilution checkerboard assay²⁷ was that the cell treatment in this study was performed in ½ PBS instead of cell culture medium, and the growth medium was added after the treatment. Our previous study showed that reaction buffers played important roles on the inactivation of bacterial cells and the cell treatment was much more effective in PBS than in broth.⁵² As for the most efficient combination in this study, the combination of 8 μg/mL CuWO₄ and 2 μg/mL CuS reduced 87.5% and 75% dosage of CuWO₄ and CuS, respectively, compared to using them separately to reach a complete killing effect. The significant dosage decrease is important on environmental health and reduces economic burden. The synergistic photocatalytic effects were also found in the hybrid composites consisting of CuWO₄ with other photocatalysts. For instance, the synergy effects were observed in the combination of CuWO₄ and TiO₂ on atrazine degradation, showing an increased degradation efficiency of 92.1% after 270 min, which was 1.94 times higher than that of TiO₂ alone.⁵³ The spatially separated cocatalysts and p-n heterojunctions in Pt/CuWO₄/Co₃O₄ photoanode system exhibited a prominently enhanced photocurrent of 4.4 mA/cm² at 1.23 V vs. RHE, demonstrating that synergistic effect of this system could effectively achieve improved photoelectrochemical

**Fig. 5** Illustration of the checkerboard assay results in a 96-well plate using CuWO₄ and CuS.**Fig. 6** Isobologram analysis for CuWO₄/CuS combination against *S. typhi* cells.

performance for water splitting.⁵⁴ The nanostructured ZnO/CuWO₄ heterojunction film had a photoelectrochemical degradation efficiency of 82% on RhB, making it approximately twice as effective as ZnO film.⁵⁵ It was also observed that the surface modification of CuWO₄ with 1.8 wt.% CuO can increase the activity by approximately 9 times under UV light and by 5 times under visible light, for phenol degradation in aerated aqueous suspension.¹⁴ Although these studies showed the synergistic effects, the authors did not show how to optimize the combination ratios. It is worth noting that the aforementioned photocatalysts such as TiO₂ and ZnO have a bandgap of 3.20⁹ and 3.37,⁴⁴ respectively, which corresponds to an absorption wavelength of 387 and 368 nm, all in the ultraviolet range. The goal of this study was to optimize the synergistic effect of visible light-driven photocatalysts for bacterial inactivation. CuS, with a visible-wavelength bandgap (1.8 eV)³⁸, is a novel candidate, and such a study using the combination of CuWO₄ and CuS has never been reported before.

3.4 Antimicrobial effects of CuWO₄/CuS hybrid composites

CuWO₄/CuS hybrid composites with varying weight ratios were used to test the effectiveness on *S. typhi*, *S. aureus*, and *B. subtilis*. The concentration of CuWO₄ and CuS for the test was determined based on the results from the checkerboard assay. The effect of the mixture consisting of 8 µg/mL CuWO₄ and 2 µg/mL CuS (denoted as 8CuWO₄/2CuS) were compared with other combinations through plating method, including hybrid composites consisting of 8 µg/mL CuWO₄ and 0.5 µg/mL CuS (8CuWO₄/0.5CuS), 8 µg/mL CuWO₄ and 1 µg/mL CuS (8CuWO₄/1CuS), 2 µg/mL CuWO₄ and 2 µg/mL CuS (2CuWO₄/2CuS), and 4 µg/mL CuWO₄ and 2 µg/mL CuS (4CuWO₄/2CuS). The testing results were consistent with the results from checkerboard assay, showing that the hybrid composite consisting of 8 µg/mL CuWO₄ and 2 µg/mL CuS was the most effective combination and killed all the tested bacteria, showing ~ 5.8 log reduction (Fig. 7). This results also proved reliability of the checkerboard assay.

B. subtilis cells were more vulnerable to the treatments than the other 2 bacterial strains and showed a complete inactivation in all the combinations except for 8CuWO₄/0.5CuS. By

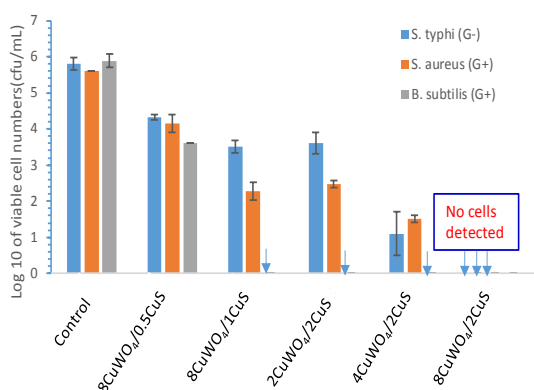


Fig. 7 Antimicrobial effects of CuWO₄/CuS combination. The numbers before the components indicate the concentration (µg/mL). Data is presented as mean values with ± SD error bars.

comparing bacteria *S. aureus* and *S. typhi*, the former were more vulnerable to the treatments than the latter in general except for the 4CuWO₄/2CuS treatment. The possible reason for the difference was that both *B. subtilis* and *S. aureus* are G⁺ bacteria, and *S. typhi* is G⁻ bacteria. G⁺ bacteria usually are more vulnerable to chemical treatments than G⁻ negative bacteria.⁵⁶ Giving an example, in 2017 the World Health Organization (WHO) published a list of antibiotic-resistant priority pathogens, and the majority on the list is G⁻ bacterial pathogens.⁵⁷ The characteristics of G⁻ bacteria being more resistant to chemicals than G⁺ bacteria are due to the cell wall structure difference. The complex G⁻ bacterial cell wall is made of multiple layers of peptidoglycans, lipoproteins, phospholipids, and lipopolysaccharides, which hampers the penetration of particles in bacterial cells.⁵⁶ The outer membrane of G⁻ bacteria is the main reason for resistance to a wide range of antibiotics including β-lactams, quinolones, colistins and other antibiotics.⁵⁶ The cell wall structure difference might be the explanation for our observation that CuWO₄/CuS combinations showed different antimicrobial effects on different bacterial strains.

The XRD pattern for CuWO₄/CuS hybrid composites did not show any deleterious phase changes after the photocatalytic bacterial inactivation experiment, as shown in Fig. S1, Supporting Information. The stability of the hybrid composites was also evidenced by EDS mapping and elemental analysis (Figs. S2 and S3, Supporting Information). The elemental compositions of the hybrid composite only changed slightly after the bacterial inactivation under white light irradiation.

3.4 Proposed mechanisms of photocatalytic inactivation of bacteria

It is generally recognized that after band gap excitation a semiconductor could generate electrons (e⁻) and holes (h⁺) in its conduction and valence bands, respectively. These charge carriers may recombine to heat or migrate onto the surface, reacting with suitable electron donors and acceptors.¹⁴ Several reactive oxygen species (ROS), such as [•]O₂⁻, H₂O₂, ¹O₂, and [•]OH, are generated through the redox reactions with dissolved oxygen and water.⁵⁸ The generation capacity of ROS is the essential factor for photocatalysis. ROS with high oxidative and reductive activities can easily degrade organic and inorganic pollutant molecules.⁵⁹ The interaction of ROS with biological microorganisms can cause direct injury to proteins, membrane lipids, and nuclei acids, leading to cell death.⁶⁰

By simply mixing CuWO₄ and CuS, synergistic antimicrobial effects were observed in the presence of visible light. The mixture of CuWO₄/CuS was similar to the structure of a traditional type-II heterojunction when the two nanopowders were in close contact. Type-II semiconductor heterojunction can be realized when one of the semiconductor's conduction and valence bands are lower than those of its neighboring semiconductor. Thus, the electrons are confined to one material and holes to the other, preventing electron-hole recombination, manifesting as a quenching of photoluminescence in the heterojunction.⁶¹

Charge transfer in the CuWO₄/CuS composite was probed via photoluminescence spectroscopy using a Raman spectrometer. The

PL spectra for CuWO₄, CuS and CuS/CuWO₄ hybrid composite with a w/w ratio of 1:4 are shown in Fig. 8. In the case of the CuWO₄/CuS hybrid composite, a strong PL quenching was observed, indicating a charge transfer at the interface of CuWO₄/CuS composite.

The possible mechanisms of photocatalytic inactivation of bacteria are shown in Fig. 9. The E_{cb} and E_{vb} values of CuWO₄ and CuS were estimated using the following expressions:⁶²

$$E_{vb} = \chi - E_0 + 0.5E_g \quad (2)$$

$$E_{cb} = E_{vb} - E_g \quad (3)$$

Where E_{vb} is the valence band (VB) edge potential, the E_0 value is constant 4.5 eV versus normal hydrogen electrode (NHE), E_{cb} is the conduction band (CB) edge potential, E_g is the bandgap of the semiconductor, and χ is the geometric mean of the electronegativities of atoms constituting the semiconductor. The VB position and CB position are estimated to be + 2.9 eV and 0.50 eV, respectively for CuWO₄,^{63,64} whereas these values, are + 1.67 eV and -0.13 eV respectively, for CuS.⁶⁵⁻⁶⁷

Under visible light irradiation, CuWO₄ and CuS could generate e^- and h^+ , and the generated e^- and h^+ could be effectively transferred to the lower potential band. The photo-induced e^- of CuS are transferred to the CB orbitals of CuWO₄, and the h^+ of the CuWO₄ are transferred to the VB orbitals of CuS. The e^- in the CB orbitals of CuWO₄ reduced O₂ to $\cdot O_2^-$, and h^+ in the VB orbitals of CuS oxidized H₂O to $\cdot OH$ and H₂O₂. The produced ROS reacted with bacteria and caused cell damage, leading to synergistic antimicrobial effects and cell death. A similar mechanism of the degradation of RhB by CuWO₄/CuS heterojunction was reported by Cui et al.²⁸ in which the formation of CuWO₄/CuS heterojunction was evidenced by the significant photoluminescence quenching.

Both CuWO₄ and CuS can generate a series of photo-induced reactive species including $\cdot OH$ and $\cdot O_2^-$ with the irradiation of visible light.^{68,69} CuWO₄ and CuS have been reported for the capabilities to effectively degrade various pollutants.^{68,69} The ROS generation by CuWO₄ could be the explanation for the antimicrobial effects in this study. The difference in band gap also allows them to function synergistically under illumination. This supports our hypothesis that interfacing these two materials could lead to superior separation and stabilization of photogenerated e^- and h^+ . Charge transfer is energetically

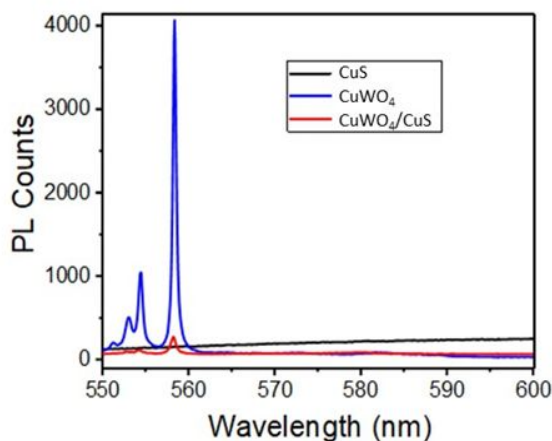


Fig. 8 PL spectra of CuS, CuWO₄, and CuWO₄/CuS hybrid composites.

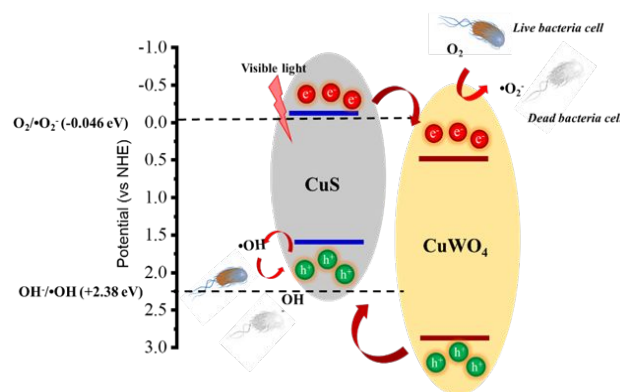


Fig. 9 Proposed mechanism of photocatalytic inactivation of bacteria by CuWO₄/CuS hybrid composite.

favorable because of the misalignment of the valence and conduction band edges.

Although individual semiconductor photocatalysts might show good photocatalytic efficiencies when the reaction condition is suitable, using a single photocatalyst may face a drawback since photogenerated e^- and h^+ pairs are generally likely to recombine, leading to reduced quantum and photocatalytic efficiencies.^{70, 71} However, this drawback can be improved by coupling with another photocatalyst which can effectively increase the separation of e^- and h^+ . The heterojunction photocatalysts typically could be grouped into six categories based on the heterojunction structure: traditional (e.g., type I, type II, and type III), p-n, Z-scheme, step-scheme, Schottky, and surface heterojunctions.^{59,72,73} In terms of traditional heterojunction system, only type II heterojunction can be an ideal system to improve the separation of e^- and h^+ . In type II heterojunctions, the e^- transfers to the semiconductor with a lower CB level. Meanwhile, the h^+ transfers to the semiconductor with a higher VB level, decreasing the contact and recombination electron-hole pairs.^{59, 74}

The photocatalytic efficiency of the photo-induced degradation varies over a wide range due to the type of photocatalysts used and the solution conditions employed.⁵⁴ Narrow bandgap, large specific surface area and efficiency of the separation of photoexcited electrons and holes were the essential factors for the enhanced photocatalytic activity.²⁸ N₂ adsorption isotherms were obtained for a) CuS, b) CuWO₄, and c) CuS/CuWO₄ hybrid composite with a w/w ratio of 1:4 (see Fig. S4 - Supporting Information). The BET surface areas for CuS, CuWO₄, and CuS/CuWO₄ hybrid composite were determined to be 0.5, 1.4, and 8.0 m²/g, respectively, confirming an increase of the surface area as a result of ultrasound-assisted physical mixing.

4. Conclusions

In this study, the checkerboard method was developed by the modification of traditional broth microdilution checkerboard assay to examine the antibacterial efficacy by CuWO₄ and CuS nanopowders individually and in mixtures of varying weight ratios. This method provided a way to find the best and most effective combination of antimicrobial photocatalysts. The

hybrid composite consisting of 8 $\mu\text{g/mL}$ CuWO_4 and 2 $\mu\text{g/mL}$ CuS was found to generate the maximum synergistic effect, showing a complete killing effect on all three bacteria with ~ 5.8 log cell reduction. The potent antimicrobial effects of CuWO_4/CuS hybrid composites made it a feasible strategy to inactivate pathogenic bacteria in the environment in a fast (in 1 h), easy, and effective manner. These findings have significant implications for the coupling of semiconductors with suitable bandgaps to develop new and effective antimicrobial materials for water disinfection.

Author Contributions

XD and FY designed this study. XD, RK, and LH performed the laboratory experiments. XD and RK evaluated the data and drafted the manuscript. BC, LY, RS, and FY revised the manuscript. All authors accepted to submit for publication.

Conflicts of interest

There are no conflicts to declare.

Acknowledgements

XD, BC, and FY are grateful for the financial support of this project by the U.S. National Science Foundation (Awards #1831133 and #2122044). This material is based upon work supported in part by the U. S. Army Research Office under contract number W911NF2210109. RK and RS thank Penn State University for funding. LH acknowledges RTI International for funding support.

References

1. E. Scallan, R. M. Hoekstra, F. J. Angulo, R. V. Tauxe, M. A. Widdowson, S. L. Roy, J. L. Jones and P. M. Griffin, Foodborne illness acquired in the United States--major pathogens, *Emerg Infect Dis*, 2011, **17**, 7-15.
2. J. H. Nakao, D. Talkington, C. A. Bopp, J. Besser, M. L. Sanchez, J. Guarisco, S. L. Davidson, C. Warner, M. G. McIntyre, J. P. Group, N. Comstock, K. Xavier, T. S. Pinsent, J. Brown, J. M. Douglas, G. A. Gomez, N. M. Garrett, H. A. Carleton, B. Tolar and M. E. Wise, Unusually high illness severity and short incubation periods in two foodborne outbreaks of *Salmonella Heidelberg* infections with potential coincident *Staphylococcus aureus* intoxication, *Epidemiol Infect*, 2018, **146**, 19-27.
3. P. R. McAdam, K. E. Templeton, G. F. Edwards, M. T. G. Holden, E. J. Feil, D. M. Aanensen, H. J. A. Bargawi, B. G. Spratt, S. D. Bentley, J. Parkhill, M. C. Enright, A. Holmes, E. K. Girvan, P. A. Godfrey, M. Feldgarden, A. M. Kearns, A. Rambaut, D. A. Robinson and J. R. Fitzgerald, Molecular tracing of the emergence, adaptation, and transmission of hospital-associated methicillin-resistant *Staphylococcus aureus*, *Proc. Natl. Acad. Sci. USA*, 2012, **109**, 9107-9112.
4. A. K. Goel, Anthrax: A disease of biowarfare and public health importance, *World J Clin Cases*, 2015, **3**, 20-33.
5. X. L. Dong, M. Al Awak, N. Tomlinson, Y. G. Tang, Y. P. Sun and L. J. Yang, Antibacterial effects of carbon dots in combination with other antimicrobial reagents, *Plos One*, 2017, **12**, e0185324.
6. N. Ding, X. M. Chang, N. Shi, X. F. Yin, F. Qi and Y. X. Sun, Enhanced inactivation of antibiotic-resistant bacteria isolated from secondary effluents by g-C₃N₄ photocatalysis, *Environ Sci Pollut R*, 2019, **26**, 18730-18738.
7. P. Lozovskis, V. Jankauskaite, A. Guobiene, V. Kareiviene and A. Vitkauskiene, Effect of graphene oxide and silver nanoparticles hybrid composite on *P. aeruginosa* strains with acquired resistance genes, *Int J Nanomed*, 2020, **15**, 5147-5163.
8. T. Matsunaga, R. Tomoda, T. Nakajima and H. Wake, Photoelectrochemical sterilization of microbial cells by semiconductor powders, *FEMS Microbiology Letters*, 1985, **29**, 211-214.
9. P. Wang, B. Huang, X. Qin, X. Zhang, Y. Dai and M. H. Whangbo, Ag/AgBr/WO₃.H₂O: visible-light photocatalyst for bacteria destruction, *Inorg Chem*, 2009, **48**, 10697-10702.
10. P. Raizada, S. Sharma, A. Kumar, P. Singh, A. A. P. Khan and A. M. Asiri, Performance improvement strategies of CuWO_4 photocatalyst for hydrogen generation and pollutant degradation, *J Environ Chem Eng*, 2020, **8**, 104230.
11. F. A. Benko, C. L. Maclaurin and F. P. Koffyberg, CuWO_4 and Cu_3WO_6 as anodes for the photoelectrolysis of Water, *Mater Res Bull*, 1982, **17**, 133-136.
12. J. E. Yourey, K. J. Pyper, J. B. Kurtz and B. M. Bartlett, Chemical stability of CuWO_4 for photoelectrochemical water oxidation, *J Phys Chem C*, 2013, **117**, 8708-8718.
13. J. C. Hill and K. S. Choi, Synthesis and characterization of high surface area CuWO_4 and Bi_2WO_6 electrodes for use as photoanodes for solar water oxidation, *J Mater Chem A*, 2013, **1**, 5006-5014.
14. H. H. Chen, W. H. Leng and Y. M. Xu, Enhanced visible-light photoactivity of CuWO_4 through a surface-deposited CuO , *J Phys Chem C*, 2014, **118**, 9982-9989.
15. B. Kavitha and R. Karthiga, Synthesis and characterization of CuWO_4 as nano-adsorbent for removal of Nile blue and its antimicrobial studies, *J. Mater. Environ. Sci.*, 2020, **11**, 57-68.
16. R. Gupta, B. Boruah, J. M. Modak and G. Madras, Kinetic study of Z-scheme $\text{C}_3\text{N}_4/\text{CuWO}_4$ photocatalyst towards solar light inactivation of mixed populated bacteria, *J Photoch Photobio A*, 2019, **372**, 108-121.
17. K. Vignesh, R. Priyanka, R. Hariharan, M. Rajarajan and A. Suganthi, Fabrication of CdS and CuWO_4 modified TiO_2 nanoparticles and its photocatalytic activity under visible light irradiation, *J Ind Eng Chem*, 2014, **20**, 435-443.
18. W. C. Xu, S. L. Zhu, Y. Q. Liang, Z. Y. Li, Z. D. Cui, X. J. Yang and A. Inoue, Nanoporous CuS with excellent photocatalytic property, *Sci Rep-Uk*, 2015, **5**, 18125.
19. Y. Liang, J. L. Zhang, H. H. Quan, P. Zhang, K. T. Xu, J. S. He, Y. C. Fang, J. C. Wang and P. T. Chen, Antibacterial effect of copper sulfide nanoparticles on infected wound healing, *Surg Infect*, 2021, **22**, 894-902.
20. E. Addae, X. L. Dong, E. McCoy, C. Yang, W. Chen and L. J. Yang, Investigation of antimicrobial activity of photothermal therapeutic gold/copper sulfide core/shell nanoparticles to bacterial spores and cells, *J Biol Eng*, 2014, **8**, 11.
21. A. Swaidan, S. Ghayyem, A. Barras, A. Addad, S. Szunerits and R. Boukherroub, Enhanced antibacterial activity of CuS-BSA/lysozyme under near infrared light irradiation, *Nanomaterials-Basel*, 2021, **11**, 2156.
22. T. P. Mofokeng, M. J. Moloto, P. M. Shumbula, P. Nyamukamba, P. K. Mubiayi, S. Takaizda and L. Marais, Antimicrobial activity of amino acid-capped zinc and copper sulphide nanoparticles, *J Nanotechnol*, 2018, **2018**, 4902675.
23. P. Raizada, A. Sudhaik, P. Singh, A. Hosseini-Bandegharaei and P. Thakur, Converting type II AgBr/VO into ternary Z scheme photocatalyst via coupling with phosphorus doped g-C₃N₄ for enhanced photocatalytic activity, *Sep Purif Technol*, 2019, **227**, 115692.
24. J. Luo, P. Lin, P. Zheng, X. Zhou, X. Ning, L. Zhan, Z. Wu, X. Liu and X. Zhou. In suit constructing S-scheme $\text{FeOOH/MgIn}_2\text{S}_4$ heterojunction with boosted interfacial charge separation and redox activity for efficiently eliminating antibiotic pollutant, *Chemosphere*, 2022, **298**, 134297.
25. J. Luo, X. Zhou, F. Yang, X. Ning, L. Zhan, Z. Wu and X. Zhou. Generating a captivating S-scheme $\text{CuBi}_2\text{O}_4/\text{CoV}_2\text{O}_6$ heterojunction with boosted charge spatial separation for efficiently removing tetracycline antibiotic from wastewater. *J. Clean. Prod.*, 2022, **357**, 131992.
26. J. Luo, J. Chen, X. Chen, X. Ning, L. Zhan and X. Zhou, Construction of cerium oxide nanoparticles immobilized on the surface of zinc vanadate nanoflowers for accelerated photocatalytic degradation of tetracycline under visible light irradiation, *J. Colloid Interface Sci.* 2021, **587**, 831-844.
27. J. A. Moody, in *Clinical microbiology procedures handbook*, ed. H. D.

- Eisenberg, American Society for Microbiology, Washington, DC., 1992, pp. 5.18.11-15.18.23.
28. Y. Y. Cui, C. C. Lin, M. K. Li, N. L. Zhu, J. J. Meng and J. T. Zhao, CuWO₄/CuS heterojunction photocatalyst for the application of visible-light-driven photodegradation of dye pollutants, *J Alloy Compd*, 2022, **893**, 162181.
 29. S. K. Pillai, R. C. Moellering Jr. and G. M. Eliopoulos, in *Antibiotics In Laboratory Medicine*, ed. V. Lorian, Lippincott Williams & Wilkins, Philadelphia, PA, 5th edn., 2005, ch. 9, pp. 365-441.
 30. Y. Cai, R. Wang, F. Pei and B. B. Liang, Antibacterial activity of allicin alone and in combination with beta-lactams against *Staphylococcus spp.* and *Pseudomonas aeruginosa*, *J Antibiot*, 2007, **60**, 335-338.
 31. X. L. Dong, A. E. Bond, N. Y. Pan, M. Coleman, Y. G. Tang, Y. P. Sun and L. J. Yang, Synergistic photoactivated antimicrobial effects of carbon dots combined with dye photosensitizers, *Int J Nanomed*, 2018, **13**, 8025-8035.
 32. G. Roks, C. L. P. Deckers, H. Meinardi, R. Dirksen, J. Van Egmond and C. M. van Rijn, Effects of polytherapy compared with monotherapy in antiepileptic drugs: An animal study, *J Pharmacol Exp Ther*, 1999, **288**, 472-477.
 33. M. Badaoui Najjar, D. Kashtanov and M. L. Chikindas, Epsilon-poly-L-lysine and nisin A act synergistically against Gram-positive food-borne pathogens *Bacillus cereus* and *Listeria monocytogenes*, *Lett Appl Microbiol*, 2007, **45**, 13-18.
 34. K. S. Kaushik, J. Stohlhandske, O. Shindell, H. D. Smyth and V. D. Gordon, Tobramycin and bicarbonate synergise to kill planktonic *Pseudomonas aeruginosa*, but antagonise to promote biofilm survival, *NPJ Biofilms Microbiomes*, 2016, **2**, 16006.
 35. H. Fjellvag, F. Gronvold, S. Stolen, A. F. Andresen, R. Mullerkafer and A. Simon, Low-temperature structural distortion in CuS, *Z Kristallogr*, 1988, **184**, 111-121.
 36. D. J. Jovanovic, I. L. Validzic, M. Mitric and J. M. Nedeljkovic, Synthesis and structural characterization of nano-sized copper tungstate particles, *Acta Chim Slov*, 2012, **59**, 70-74.
 37. A. Escobedo-Morales, I. I. Ruiz-Lopez, M. D. Ruiz-Peralta, L. Tepech-Carrillo, M. Sanchez-Cantu and J. E. Moreno-Orea, Automated method for the determination of the band gap energy of pure and mixed powder samples using diffuse reflectance spectroscopy, *Heliyon*, 2019, **5**, e01505.
 38. A. E. B. Lima, M. J. S. Costa, R. S. Santos, N. C. Batista, L. S. Cavalcante, E. Longo and G. E. Luz, Facile preparation of CuWO₄ porous films and their photoelectrochemical properties, *Electrochim Acta*, 2017, **256**, 139-145.
 39. S. Gunalan, R. Sivaraj and V. Rajendran, Green synthesized ZnO nanoparticles against bacterial and fungal pathogens, *Prog Nat Sci-Mater*, 2012, **22**, 695-702.
 40. M. Thiruppathi, J. V. Kumar, M. Vahini, C. Ramalingan and E. R. Nagarajan, A study on divergent functional properties of sphere-like CuWO₄ anchored on 2D graphene oxide sheets towards the photocatalysis of ciprofloxacin and electrocatalysis of methanol, *J Mater Sci-Mater El*, 2019, **30**, 10172-10182.
 41. F. Ahmadi, M. Rahimi-Nasrabadi and M. Eghbali-Arani, The synthesis of CuWO₄ nano particles by a new morphological control method, characterization of its photocatalytic activity, *J Mater Sci-Mater El*, 2017, **28**, 5244-5249.
 42. A. Rashidizadeh, H. Ghafari and Z. Rezazadeh, Improved visible-light photocatalytic activity of g-C₃N₄/CuWO₄ nanocomposite for degradation of methylene blue, *MDPI Proceedings*, 2020, **41**, 43.
 43. W. C. Ding, X. N. Wu and Q. F. Lu, Structure and photocatalytic activity of thin-walled CuWO₄ nanotubes: An experimental and DFT study, *Mater Lett*, 2019, **253**, 323-326.
 44. T. Mavric, M. Valant, M. Forster, A. J. Cowan, U. Lavrencic and S. Emin, Design of a highly photocatalytically active ZnO/CuWO₄ nanocomposite, *J Colloid Interf Sci*, 2016, **483**, 93-101.
 45. A. Giachino and K. J. Waldron, Copper tolerance in bacteria requires the activation of multiple accessory pathways. *Mol Microbiol* 2020, **114**, 377-390.
 46. C. Malarkodi and S. Rajeshkumar, In vitro bactericidal activity of biosynthesized CuS nanoparticles against UTI-causing pathogens, *Inorg Nano-Met Chem*, 2017, **47**, 1290-1297.
 47. J. Huang, J. Zhou, J. Zhuang, H. Gao, D. Huang, L. Wang, W. Wu, Q. Li, D. P. Yang and M. Y. Han, Strong Near-Infrared Absorbing and Biocompatible CuS nanoparticles for rapid and efficient photothermal ablation of Gram-positive and -negative bacteria, *ACS Appl Mater Interfaces*, 2017, **9**, 36606-36614.
 48. D. Ayodhya and G. Veerabhadram, Preparation, characterization, photocatalytic, sensing and antimicrobial studies of *Calotropis gigantea* leaf extract capped CuS NPs by a green approach, *J Inorg Organomet P*, 2017, **27**, S215-S230.
 49. P. Dibrov, J. Dzioba, K. K. Gosink and C. C. Hase, Chemiosmotic mechanism of antimicrobial activity of Ag⁺ in *Vibrio cholerae*, *Antimicrob Agents Ch*, 2002, **46**, 2668-2670.
 50. X. J. Xu, L. Xu, G. J. Yuan, Y. M. Wang, Y. Q. Qu and M. J. Zhou, Synergistic combination of two antimicrobial agents closing each other's mutant selection windows to prevent antimicrobial resistance, *Sci Rep-Uk*, 2018, **8**, 7237.
 51. J. B. Fitzgerald, B. Schoeberl, U. B. Nielsen and P. K. Sorger, Systems biology and combination therapy in the quest for clinical efficacy, *Nat Chem Biol*, 2006, **2**, 458-466.
 52. X. L. Dong, M. Al Awak, P. Wang, Y. P. Sun and L. J. Yang, Carbon dot incorporated multi-walled carbon nanotube coated filters for bacterial removal and inactivation, *Rsc Adv*, 2018, **8**, 8292-8301.
 53. D. W. He, Y. Yang, J. J. Tang, K. G. Zhou, W. Chen, Y. Q. Chen and Z. J. Dong, Synergistic effect of TiO₂-CuWO₄ on the photocatalytic degradation of atrazine, *Environ Sci Pollut R*, 2019, **26**, 12359-12367.
 54. Z. F. Liu, Q. G. Song, M. Zhou, Z. G. Guo, J. H. Kang and H. Y. Yan, Synergistic enhancement of charge management and surface reaction kinetics by spatially separated cocatalysts and p-n heterojunctions in Pt/CuWO₄/Co₃O₄ photoanode, *Chem Eng J*, 2019, **374**, 554-563.
 55. J. P. C. Moura, R. Y. N. Reis, A. E. B. Lima, R. S. Santos and G. E. Luz, Improved photoelectrocatalytic properties of ZnO/CuWO₄ heterojunction film for RhB degradation, *J Photoch Photobio A*, 2020, **401**, 112778.
 56. Z. Breijyeh, B. Jubeh and R. Karaman, Resistance of Gram-negative bacteria to current antibacterial agents and approaches to resolve it, *Molecules*, 2020, **25**, 1340.
 57. G. V. Asokan, T. Ramadhan, E. Ahmed and H. Sanad, WHO global priority pathogens list: a bibliometric analysis of Medline-PubMed for knowledge mobilization to infection prevention and control practices in Bahrain, *Oman Med J*, 2019, **34**, 184-193.
 58. Y. Nosaka and A. Y. Nosaka, Generation and detection of reactive oxygen species in photocatalysis, *Chem Rev*, 2017, **117**, 11302-11336.
 59. X. H. He, T. H. Kai and P. Ding, Heterojunction photocatalysts for degradation of the tetracycline antibiotic: a review, *Environ Chem Lett*, 2021, **19**, 4563-4601.
 60. I. S. Arts, A. Gennaris and J. F. Collet, Reducing systems protecting the bacterial cell envelope from oxidative damage, *Febs Lett*, 2015, **589**, 1559-1568.
 61. X. Hong, J. Kim, S.-F. Shi, Y. Zhang, C. Jin, Y. Sun, S. Tongay, J. Wu, Y. Zhang and F. Wang, Ultrafast charge transfer in atomically thin MoS₂/WS₂ heterostructures, *Nat. Nanotechnol.* 2014, **9**, 682-686.
 62. N. Jatav, J. Kuntail, D. Khan, A. Kumar De and I. Sinha, AgI/CuWO₄ Z-scheme photocatalyst for the degradation of organic pollutants: Experimental and molecular dynamics studies, *J. Colloid Interface Sci.* 2021, **599**, 717-729.
 - 63.. K. Li, C. Zhang, X. Li, Y. Du, P. Yang and M. Zhu, A nanostructured CuWO₄/Mn₃O₄ with p/n heterojunction as photoanode toward enhanced water oxidation, *Catal. Today*. 2019, **335**, 173-179.
 64. A.E.B. Lima, M. Assis, A.L.S. Resende, H.L.S. Santos, L.H. Mascaro, E. Longo, R.S. Santos, L.S. Cavalcante and G.E. Luz, CuWO₄|MnWO₄ heterojunction thin film with improved photoelectrochemical and photocatalytic properties using simulated solar irradiation, *J. Solid State Electrochem.* 2022, **26**, 997-1011.
 65. A. Prakash, M. Dan, S. Yu, S. Wei, Y. Li, F. Wang and Y. Zhou, In₂S₃/CuS nanosheet composite: An excellent visible light photocatalyst for H₂ production from H₂S, *Sol. Energy Mater. Sol. Cells*. 2018, **180**, 205-212.
 66. L. Guo, K. Zhang, X. Han, Q. Zhao, D. Wang and F. Fu, 2D In-plane CuS/Bi₂WO₆ p-n heterostructures with promoted visible-light-driven photo-fenton degradation performance, *Nanomaterials*. 2019, **9**, 1151.
 67. Q. Chen, M. Zhang, J. Li, G. Zhang, Y. Xin and C. Chai, Construction of immobilized 0D/1D heterostructure photocatalyst Au/CuS/CdS/TiO₂ NBs with enhanced photocatalytic activity towards moxifloxacin degradation, *Chem. Eng. J.* 2020, **389**, 124476

- 1
2
3 68. L. M. Liang, H. Liu, Y. Tian, Q. Y. Hao, C. C. Liu, W. C. Wang and X. J. Xie,
4 Fabrication of novel CuWO₄ hollow microsphere photocatalyst for dye
5 degradation under visible-light irradiation, *Mater Lett*, 2016, **182**, 302-
6 304.
- 7 69. S. Adhikari, D. Sarkar and G. Madras, Hierarchical design of CuS
8 architectures for visible light photocatalysis of 4-chlorophenol, *ACS*
9 *Omega*, 2017, **2**, 4009-4021.
- 10 70. B. Louangsouphom, X. J. Wang, J. K. Song and X. Wang, Low-temperature
11 preparation of a N-TiO₂/macroporous resin photocatalyst to degrade
12 organic pollutants, *Environ Chem Lett*, 2019, **17**, 1061-1066.
- 13 71. T. Soltani, A. Tayyebi and B. K. Lee, Photolysis and photocatalysis of
14 tetracycline by sonochemically heterojunctioned BiVO₄/reduced
15 graphene oxide under visible-light irradiation, *J Environ Manage*, 2019,
16 **232**, 713-721.
- 17 72. X. H. He, A. Z. Wang, P. Wu, S. B. Tang, Y. Zhang, L. Li and P. Ding,
18 Photocatalytic degradation of microcystin-LR by modified TiO₂
19 photocatalysis: A review, *Sci Total Environ*, 2020, **743**, 140694.
- 20 73. X. R. Yang, Z. Chen, W. Zhao, C. X. Liu, X. X. Qian, M. Zhang, G. Y. Wei, E.
21 Khan, Y. H. Ng and Y. S. Ok, Recent advances in photodegradation of
22 antibiotic residues in water, *Chem Eng J*, 2021, **405**, 126806.
- 23 74. H. L. Zhou, Y. Q. Qu, T. Zeid and X. F. Duan, Towards highly efficient
24 photocatalysts using semiconductor nanoarchitectures, *Energ Environ Sci*,
25 2012, **5**, 6732-6743.
- 26
27
28
29
30
31
32
33
34
35
36
37
38
39
40
41
42
43
44
45
46
47
48
49
50
51
52
53
54
55
56
57
58
59
60